



Investigation of $(\text{CeO}_2)_x(\text{Sc}_2\text{O}_3)_{(0.11-x)}(\text{ZrO}_2)_{0.89}$ ($x = 0.01-0.10$) electrolyte materials for intermediate-temperature solid oxide fuel cell

Man Liu, Changrong He, Jianxin Wang, Wei Guo Wang**, Zhenwei Wang*

Ningbo Institute of Material Technology and Engineering, Chinese Academy of Sciences, 519 Zhuangshi Road, Ningbo, Zhejiang 315201, China

ARTICLE INFO

Article history:

Received 26 October 2009

Received in revised form

21 December 2009

Accepted 21 December 2009

Available online 28 December 2009

Keywords:

Solid oxide fuel cell

Electrolyte

Oxide ionic conductivity

Scandia-stabilized zirconia

Sintering aid

ABSTRACT

Oxide ionic conductivities of $(\text{CeO}_2)_x(\text{Sc}_2\text{O}_3)_{(0.11-x)}(\text{ZrO}_2)_{0.89}$ ($x = 0.01-0.10$) electrolytes were optimized for the application in intermediate-temperature solid oxide fuel cell (IT-SOFC). Powders with different contents of CeO_2 and Sc_2O_3 were prepared via a co-precipitation method. The obtained powders and pellets were characterized by X-ray diffraction (XRD), scanning electron microscopy (SEM), energy dispersive spectroscopy (EDS) and impedance spectroscopy. Among all the compositions, $(\text{CeO}_2)_{0.04}(\text{Sc}_2\text{O}_3)_{0.07}(\text{ZrO}_2)_{0.89}(4\text{Ce}7\text{ScZr})$ gives the highest ionic conductivity of 0.065 S cm^{-1} at 800°C . The effects on densification and electrical properties of different sintering additives, such as SiO_2 , MgO , Co_3O_4 , MoO_3 and Bi_2O_3 , were studied and different conducting behavior with these additives were observed. The densification temperatures of CeO_2 and Sc_2O_3 co-doped electrolytes can be reduced by around 280°C with the addition of 1 mol% of Bi_2O_3 , while the electrical properties of the electrolytes are not significantly affected by the introduction of Bi_2O_3 aid.

© 2010 Elsevier B.V. All rights reserved.

1. Introduction

Anode-supported solid oxide fuel cell with thin yttria-stabilized zirconia (YSZ, 8 mol% Y_2O_3) as electrolyte is the mainstream for the operation in intermediate-temperature range ($600-800^\circ\text{C}$) [1–5]. However, the cell performance is too low when the cell runs below 700°C . Developing new solid electrolytes with higher ionic conductivity for lower temperature application is necessary [6,7].

Among zirconia-based electrolytes, scandia-stabilized zirconia (ScSZ) is a very promising candidate because it shows appropriate thermal expansion, good mechanical properties and the highest oxide ionic conductivity due to the similar ionic radius of the Sc^{3+} dopant to that of the Zr^{4+} host $R = r_{\text{Sc}^{3+}}/r_{\text{Zr}^{4+}} = 1.03$ [8,9]. Generally speaking, larger dopants, such as CeO_2 [10,11] and Y_2O_3 [7,10–15], is helpful to stabilize the cubic/tetragonal phase structure of ScSZ electrolyte down to room temperature. It was reported that the sample with 10 mol% of Sc_2O_3 and 1 mol% of CeO_2 (1Ce10ScZr) exhibits the best oxide ionic conductivity and good stability during extended annealing period [11], where the 1 mol% CeO_2 is used as phase stabilizer as usual. However, as we know there is no reported investigation carried out to optimize the best ratio of $\text{CeO}_2/\text{Sc}_2\text{O}_3$.

The sintering activity of ScSZ electrolyte is quite poor due to the similar ionic radius of Sc^{3+} and Zr^{4+} . Achieving full density by conventional sintering methods requires high sintering temperatures (up to about 1600°C). The high temperature sintering results in microstructures with grain sizes in the micron range, which subsequently induces poor mechanical stability. Higher densification temperature of ScSZ than that of YSZ is also an obstacle for its application in SOFCs. It is desirable to use lower temperature sintering which is more compatible to obtain appropriate anode microstructures.

In this paper, the ratios of CeO_2 to Sc_2O_3 of $(\text{CeO}_2)_x(\text{Sc}_2\text{O}_3)_{(0.11-x)}(\text{ZrO}_2)_{0.89}$ ($x = 0.01-0.10$) were investigated in order to obtain the best conducting electrolyte for IT-SOFCs. The structure and conductivity of the powders and pellets were investigated in detail with XRD, SEM, EDS and impedance spectroscopy. In addition, SiO_2 , MgO , Co_3O_4 [16], MoO_3 and Bi_2O_3 [17] were adopted as sintering aids for the optimized electrolyte $(\text{CeO}_2)_{0.04}(\text{Sc}_2\text{O}_3)_{0.07}(\text{ZrO}_2)_{0.89}$ in order to improve the sintering properties.

2. Experimental

2.1. Powder synthesis

High purity $\text{Ce}(\text{NO}_3)_3 \cdot 6\text{H}_2\text{O}$, $\text{Zr}(\text{OH})_4$, $\text{Bi}(\text{OH})_3$, SiO_2 , $\text{Mg}(\text{OH})_2$, $\text{Co}(\text{NO}_3)_2 \cdot 6\text{H}_2\text{O}$, MoO_3 were used as starting materials as purchased from Sinopharm Chemical Reagent Co., Ltd. Sc_2O_3 was purchased from Rare-Chem Hi-Tech Corporation of China.

The co-precipitation method was adopted to prepare powders as reported [7,11]. The stock solution was prepared by dissolving stoichiometric $\text{Zr}(\text{OH})_4$ and

* Corresponding author. Tel.: +86 574 86685139; fax: +86 574 87910728.

** Corresponding author. Tel.: +86 574 87911363; fax: +86 574 87911363.

E-mail addresses: wgwang@nimte.ac.cn (W.G. Wang),

zhwwang@nimte.ac.cn (Z. Wang).

Table 1
Sintering conditions and relative densities.

Sample nomenclature	Composition	Sintering condition	Relative density (%)
10Ce1ScZr	(CeO ₂) _{0.10} (Sc ₂ O ₃) _{0.01} (ZrO ₂) _{0.89}	1580 °C (10 h)	97.7
9Ce2ScZr	(CeO ₂) _{0.09} (Sc ₂ O ₃) _{0.02} (ZrO ₂) _{0.89}	1580 °C (10 h)	97.0
8Ce3ScZr	(CeO ₂) _{0.08} (Sc ₂ O ₃) _{0.03} (ZrO ₂) _{0.89}	1580 °C (10 h)	102.0
7Ce4ScZr	(CeO ₂) _{0.07} (Sc ₂ O ₃) _{0.04} (ZrO ₂) _{0.89}	1580 °C (10 h)	95.3
6Ce5ScZr	(CeO ₂) _{0.06} (Sc ₂ O ₃) _{0.05} (ZrO ₂) _{0.89}	1580 °C (10 h)	98.9
5Ce6ScZr	(CeO ₂) _{0.05} (Sc ₂ O ₃) _{0.06} (ZrO ₂) _{0.89}	1580 °C (10 h)	97.8
4Ce7ScZr	(CeO ₂) _{0.04} (Sc ₂ O ₃) _{0.07} (ZrO ₂) _{0.89}	1500 °C (10 h)	99.4
3Ce8ScZr	(CeO ₂) _{0.03} (Sc ₂ O ₃) _{0.08} (ZrO ₂) _{0.89}	1580 °C (10 h)	100.4
2Ce9ScZr	(CeO ₂) _{0.02} (Sc ₂ O ₃) _{0.09} (ZrO ₂) _{0.89}	1580 °C (10 h)	100.4
1Ce10ScZr	(CeO ₂) _{0.01} (Sc ₂ O ₃) _{0.10} (ZrO ₂) _{0.89}	1580 °C (10 h)	100.0

Sc₂O₃ in hot nitric acid. The required quantity of Ce(NO₃)₃·6H₂O was then added to the solution. Precipitation was carried out by adding ammonia to the solution under vigorously stirring. The pH value was controlled within 9–10 at the end with a pH detector. After pumping filtration, the precipitate was rinsed thoroughly with hot alcohol until most of the ammonia and water was eliminated during heating and finally dried in an oven at 110 °C for 24 h. In the case of the samples containing sintering additive, the additive was mixed with the stock solutions before co-precipitation. The powders obtained from the co-precipitation method were calcined, and then planetary ball milled with zirconia balls for 24 h. The obtained powders were uniaxially pressed into discs with a diameter of 8 mm and a thickness of 1–2 mm under 300 MPa. The pressed pellets were then sintered at a certain temperature from 1300 °C to 1580 °C, most for 10 h and some for 5 h.

2.2. Powder characterization

Phase structures of powders were characterized using XRD technique and the data were collected using a Bruker D8 Advance (Germany) with Cu K α radiation at a step of 0.02° s⁻¹ in the range of 2 θ from 20° to 80°. The sintered pellets were observed by SEM (Hitachi, S-4800, Japan). The relative density of the sintered pellets was determined via Archimedes' method. The oxide ionic conductivity of the pellets was measured using a frequency response analyzer (FRA, Solartron 1260) over a frequency range of 0.1 Hz to 1 MHz at temperature range of 450–850 °C in air with Pt electrodes. The ionic conductivity, σ , was calculated from the impedance data and the activation energy (E_a) of the conductivity was determined by the Arrhenius law:

$$\sigma T = \sigma_0 \exp\left(\frac{-E_a}{kT}\right)$$

where σ_0 was the pre-exponential factor and k was the Boltzmann constant.

Table 1 gives the nomenclature, sintering temperature and relative density of all samples.

3. Results and discussions

Fig. 1 gives XRD patterns for the powders with different ratios of CeO₂ to Sc₂O₃. As reported previously [8], 1 mol% of CeO₂ additive is sufficient for the stabilization of cubic phase of scandia-stabilized

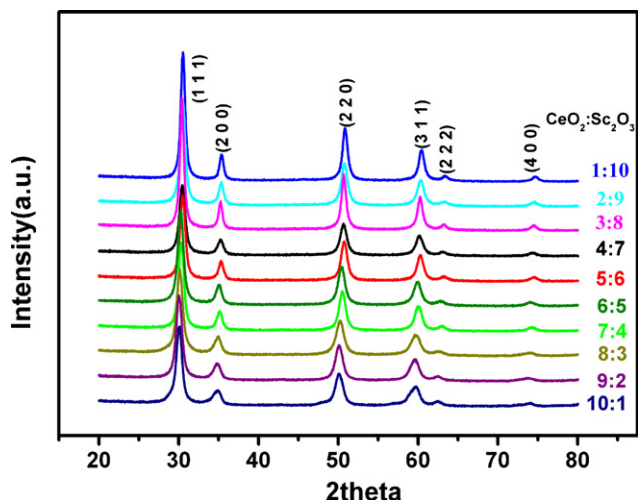


Fig. 1. XRD patterns of sintered (CeO₂)_x(Sc₂O₃)_{0.11-x}(ZrO₂)_{0.89} ($x = 0.01$ – 0.10).

zirconia at high temperatures. Increasing the content of CeO₂ thereafter does not induce additional phase. This is important for practical application as electrolytes for SOFC.

Fig. 2 compares the resistance contributions from the bulk and grain boundaries of each sample obtained at 450 °C. The total resistances of all sintered specimens vary with the doping amount of CeO₂. The grain boundary resistances are much smaller compare to the bulk resistances in all samples. The low but relatively constant values of the grain boundary resistances show that the grain boundaries are free of the segregation of resistant impurity [7].

Fig. 3 gives the ionic conductivities of all the specimens tested at 800 °C. Each point in this graph is calculated by averaging at least two measurements for the sample. 4Ce7ScZr shows the highest conductivity (0.065 S cm⁻¹ at 800 °C). The conductivity of traditional electrolyte YSZ was also tested and the values of 4Ce7ScZr are higher than that of YSZ over the whole investigation temperature range, as shown in Fig. 4. When Sc₂O₃ is co-doped with Y₂O₃ at a total amount of 11 mol%, 2Y9ScZr gives the maximum conductivity (0.0589 S cm⁻¹, 800 °C) [15]. In this study, considering the high cost of Sc₂O₃, we achieve a higher ionic conductivity with less amount of Sc₂O₃ for the future mass production. Consistent with Fig. 2, a strange drop in the conductivity is observed at 5Ce6ScZr and ionic conductivity increases with the increasing CeO₂ at low content but decreases with the increasing CeO₂ at high content. This observation is also found in (Y₂O₃)_x(Sc₂O₃)_{0.11-x}(ZrO₂)_{0.89} electrolyte material, with an inconsistency at the middle point 5.5Y5.5ScZr [15]. The reason is not fully understood.

Other than the conductivity, sintering property of scandia-stabilized zirconia is an important issue. As shown in Table 1, the achievement of density as high as above 95% for all the specimens

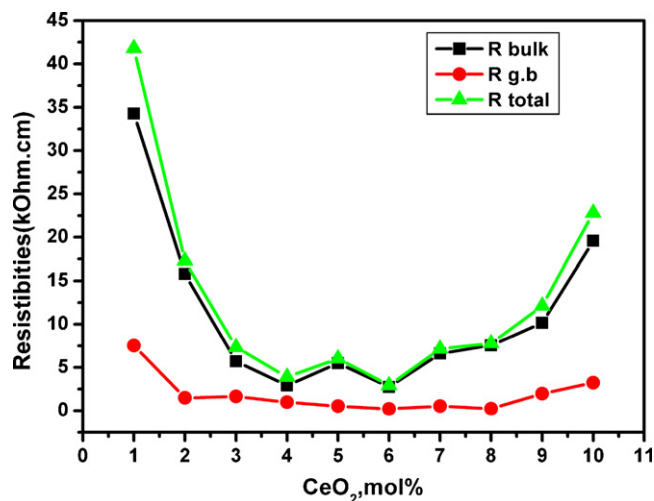


Fig. 2. Total, bulk and grain boundary resistivities of the (CeO₂)_x(Sc₂O₃)_{0.11-x}(ZrO₂)_{0.89} ($x = 0.01$ – 0.10) system as a function of the CeO₂ content, recorded at 450 °C.

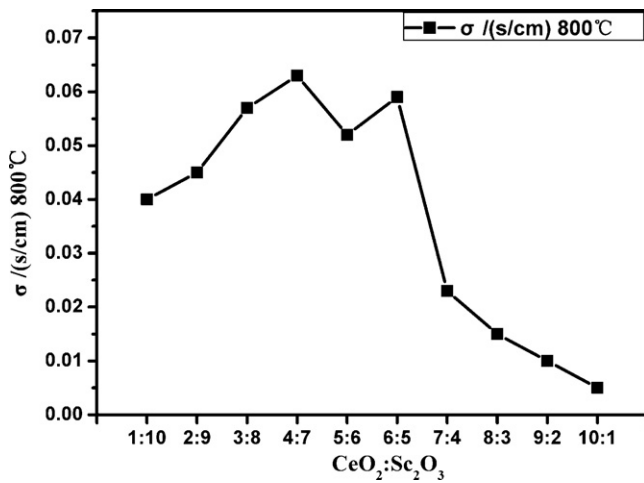


Fig. 3. Ionic conductivity of the $(\text{CeO}_2)_x(\text{Sc}_2\text{O}_3)_{0.11-x}(\text{ZrO}_2)_{0.89}$ ($x = 0.01\text{--}0.10$) system, recorded at 800°C .

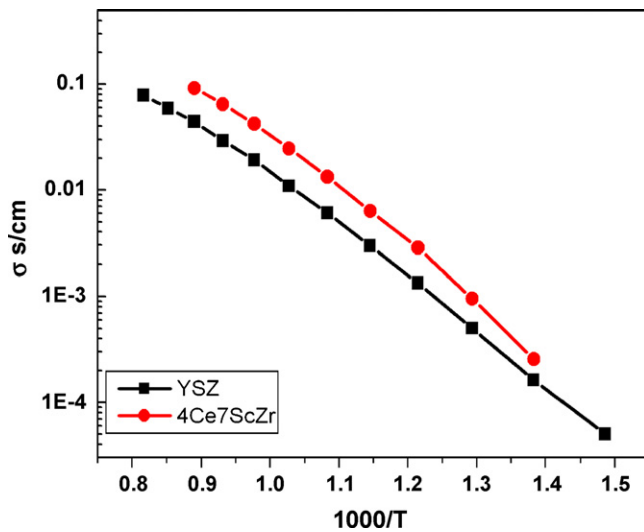


Fig. 4. Arrhenius plots of YSZ and 4Ce7ScZr.

without sintering aids requires high temperatures over 1580°C for 10 h. Lower sintering temperature results in lower density.

In order to lower the desintering temperature, SiO_2 , MgO , Co_3O_4 [16], MoO_3 and Bi_2O_3 [17] are introduced into the sample $1\text{Ce}10\text{ScZr}$ as potential sintering additives. Table 2 summarizes the sintering conditions and sample densities. With the introduction of Co_3O_4 and Bi_2O_3 , the sample can reach full densification at a temperature as low as 1300°C . The introduction of SiO_2 , MgO and

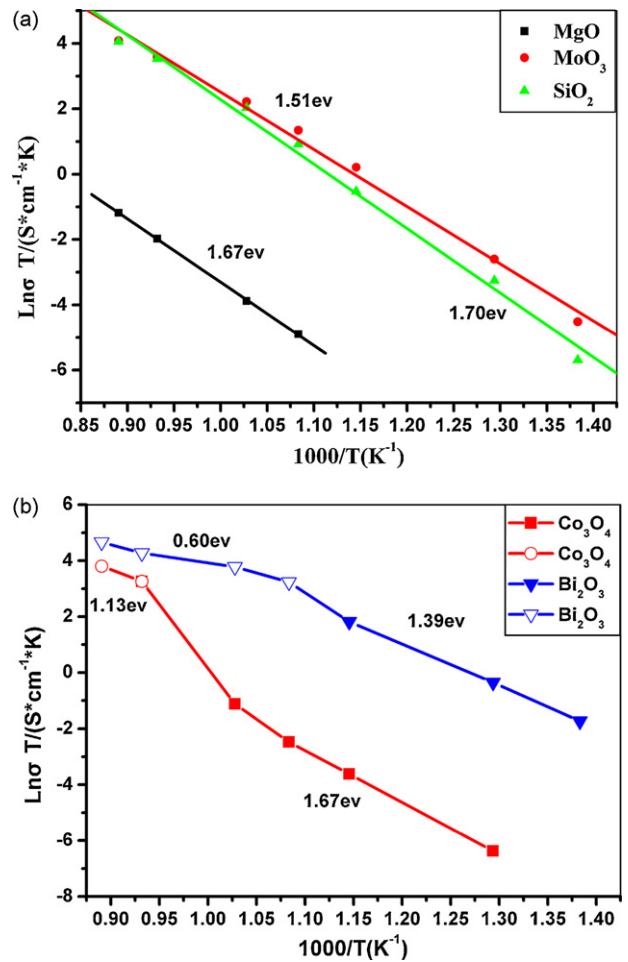


Fig. 5. Conductivity-temperature plots of specimens with introduction of different sintering additives. (a) One stage kind and (b) two stages kind.

MoO_3 results in a slightly lower density even though the samples are also sintered at 1580°C .

Fig. 5 gives the ionic conductivity behavior of the electrolytes with different sintering additive. These five sintering additives can be divided into two categories according to their performances: one stage and two stages. SiO_2 , MgO and MoO_3 belong to the one stage group because the conductivity-temperature plots of the specimen are all in a straight line. Meanwhile, Co_3O_4 and Bi_2O_3 are grouped to the two-stages group. The samples with SiO_2 , MgO and MoO_3 give higher E_a than the samples with Co_3O_4 and Bi_2O_3 and thus have lower conductivities. Therefore, SiO_2 , MgO and MoO_3 are not suitable sintering aids. As for Bi_2O_3 , liquid Bi_2O_3 appears at above 650°C , which accelerates the conduction of oxygen vacancy, and the electrolyte show different conduct-

Table 2

Sintering properties for $1\text{Ce}10\text{ScZr}$ with different sintering additives.

Sample nomenclature	Composition	Sintering condition	Relative density(%)
1Ce10ScZr-1300	1 mol% CeO_2 + 10 mol% Sc_2O_3 + 89 mol% ZrO_2	1300°C (10 h)	83
1Ce10ScZr-1400	1 mol% CeO_2 + 10 mol% Sc_2O_3 + 89 mol% ZrO_2	1400°C (10 h)	90
1Ce10ScZr-1500	1 mol% CeO_2 + 10 mol% Sc_2O_3 + 89 mol% ZrO_2	1500°C (10 h)	96
1Ce10ScZr-1580	1 mol% CeO_2 + 10 mol% Sc_2O_3 + 89 mol% ZrO_2	1580°C (10 h)	100
1Ce10ScZr-Si-1580	(1 mol% CeO_2 + 10 mol% Sc_2O_3 + 89 mol% ZrO_2) + 0.5 mol% SiO_2	1580°C (10 h)	96
1Ce10ScZr-Mg-1580	(1 mol% CeO_2 + 10 mol% Sc_2O_3 + 89 mol% ZrO_2) + 5 mol% MgO	1580°C (10 h)	92
1Ce10ScZr-Mo-1580	(1 mol% CeO_2 + 10 mol% Sc_2O_3 + 89 mol% ZrO_2) + 5 mol% MoO_3	1580°C (10 h)	96
1Ce10ScZr-Co-1300	(1 mol% CeO_2 + 10 mol% Sc_2O_3 + 89 mol% ZrO_2) + 2 mol% Co_3O_4	1300°C (10 h)	100
1Ce10ScZr-0.5Bi	(1 mol% CeO_2 + 10 mol% Sc_2O_3 + 89 mol% ZrO_2) + 0.5 mol% Bi_2O_3	1300°C (5 h)	98
1Ce10ScZr-1Bi	(1 mol% CeO_2 + 10 mol% Sc_2O_3 + 89 mol% ZrO_2) + 1 mol% Bi_2O_3	1300°C (5 h)	101
1Ce10ScZr-3Bi	(1 mol% CeO_2 + 10 mol% Sc_2O_3 + 89 mol% ZrO_2) + 3 mol% Bi_2O_3	1300°C (5 h)	100

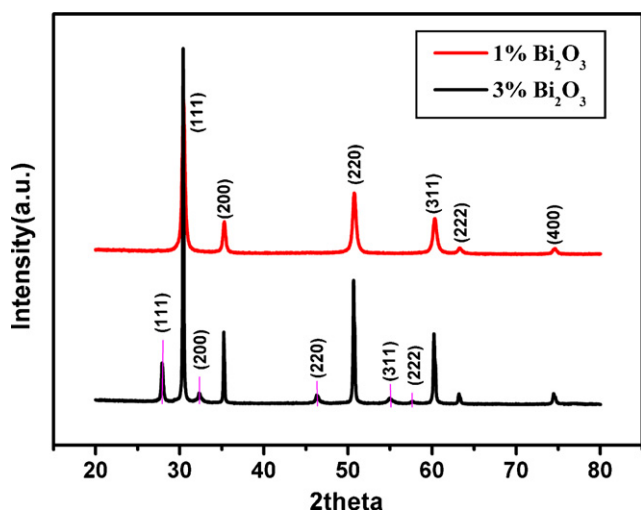


Fig. 6. XRD patterns of 1Ce10ScZr-1Bi and 11Ce10ScZr-3Bi.

ing mechanisms compared with the one at lower temperature. For Co_3O_4 , it is decomposed partially to CoO with O element released above 700°C . An endothermic peak can be detected by thermal analysis. The decomposition significantly accelerates the vacancy conduction. Therefore, two stages with different E_a appear in the conductivity–temperature curves of electrolytes with Bi_2O_3 and Co_3O_4 . The introduction of Bi_2O_3 does not change the ionic conductivity of 1Ce10ScZr (0.040 S cm^{-1} , 800°C) obviously. However, the introduction of Co_3O_4 lowers the ionic conductivity of the sample.

The effect of the Bi_2O_3 amount on conductivity is also investigated. When 0.5 mol% Bi_2O_3 is added, the diffusion of Bi_2O_3 in the sample is not enough and inhomogeneous, which can be observed by eyes. As a result, a slightly lower density is observed. 1 mol% Bi_2O_3 is necessary in order to ensure the homogenous distribution, which resulted in a fully dense sample. When 3 mol% Bi_2O_3 is used, new peaks for face-centered cubic phase of Bi_2O_3 can be detected by XRD, as shown in Fig. 6. As a result, the ionic conductivity at 800°C of 1Ce10ScZr-3Bi is lowered to 0.036 S cm^{-1} , showing a 10% drop from 0.040 S cm^{-1} of 1Ce10ScZr-1Bi. Therefore, 1 mol% Bi_2O_3 addition is chosen as an optimal amount for CeScZr electrolyte.

In our study, 1 mol% Bi_2O_3 is also used in the best composition 4Ce7ScZr, as shown in Fig. 3. The ionic conductivity of 4Ce7ScZr-1Bi is 0.067 S cm^{-1} at 800°C , which is close to 0.065 S cm^{-1} for 4Ce7ScZr. However, 4Ce7ScZr-1Bi can be fully densified at 1300°C other than 1580°C .

Fig. 7 shows the SEM micrographs of the cross-section and surface of 1Ce10ScZr-1Bi. The grain boundary on the surface is unclear and the grain size is as large as $6\ \mu\text{m}$ even sintered at 1300°C . This is due to the liquid sintering mechanism. In grain boundaries, some small particles can be found as marked in Fig. 7b. Table 3 lists the data of elemental analysis by EDS of these small particles. Higher Bi_2O_3 content can be observed in the marked area than other, suggesting Bi_2O_3 agglomeration at grain boundary. Densi-

Table 3
Elemental analyses by EDS of the selected area of 1Ce10ScZr-1Bi sintered at 1300°C for 5 h.

Element	Wt%	At%
CK	9.61	29.55
OK	15.80	36.45
ZrL	56.18	22.74
BiM	1.79	0.32
ScK	11.77	9.66
CeL	4.85	1.28

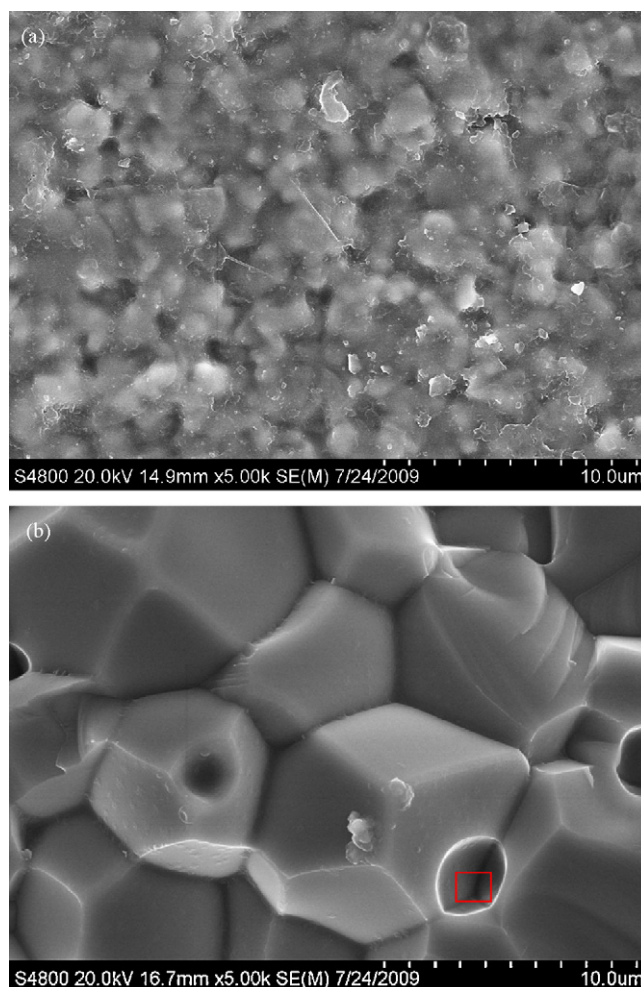


Fig. 7. SEM and of 1Ce10ScZr-1Bi at 1300°C for 5 h: (a) surface and (b) cross-section.

fication mechanism is mainly due to the characteristics change at grain boundary instead of lattice structure [18]. As confirmed by EDS map in Fig. 8, the concentration of Zr element decrease obviously at the contact part of several grains, thereby leading to a relative increase of Bi, Sc and Ce concentration.

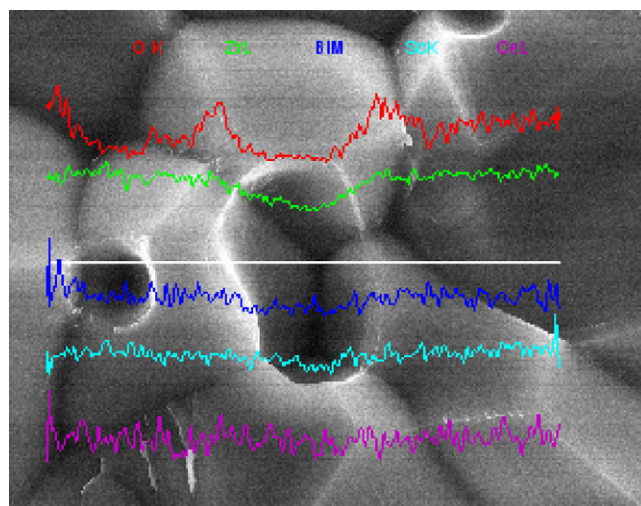


Fig. 8. EDS maps of a selected area of 1Ce10ScZr-1Bi at 1300°C for 5 h.

4. Conclusions

In this work, $(\text{CeO}_2)_x(\text{Sc}_2\text{O}_3)_{(0.11-x)}(\text{ZrO}_2)_{0.89}$ ($x = 0.01-0.10$) with various ratios of CeO_2 to Sc_2O_3 were synthesized and characterized. $4\text{Ce}7\text{ScZr}$ shows the maximum conductivity of 0.065 S cm^{-1} at 800°C , which can be a good candidate for IT-SOFCs. Bi_2O_3 is proven to be a good sintering aid to synthesize scandia-stabilized zirconia. 1 mol% of Bi_2O_3 addition to the electrolyte can reduce the densification temperature greatly and does not affect the ionic conductivity significantly. $4\text{Ce}7\text{ScZr}$ with 1 mol% addition of Bi_2O_3 is promising as the electrolyte candidate for IT-SOFC.

Acknowledgements

This work was financially supported by the National High-Tech Research and Development Program of China (863 Program, Grant No. 2007AA05Z140), Special President Founding of NIMTE and Ningbo Natural Science Foundation (Grant No. 2009A610038). Authors are also grateful for the English revision from Professor Cheng Xu and Professor Shenghu Zhou.

References

- [1] J. Ding, J. Liu, W.M. Guo, J. Alloy Compd. 480 (2009) 286–290.
- [2] Y.J. Leng, S.H. Chan, K.A. Khor, S.P. Jiang, Int. J. Hydrogen Energy 29 (2004) 1025–1033.
- [3] J.H. Kim, R.H. Song, K.S. Song, S.H. Hyun, D.R. Shin, H. Yokokawa, J. Power Sources 122 (2003) 138–143.
- [4] Y.J. Leng, S.H. Chan, K.A. Khor, S.P. Jiang, P. Cheang, J. Power Sources 117 (2003) 26–34.
- [5] J.W. Fergus, J. Power Sources 162 (2006) 30–40.
- [6] S.P.S. Badwal, F.T. Ciacchi, D. Milosevic, Solid State Ionics 136–137 (2000) 91–99.
- [7] S.P.S. Badwal, F.T. Ciacchia, S. Rajendran, J. Drennan, Solid State Ionics 109 (1998) 167–186.
- [8] D.-S. Lee, W.-S. Kim, S.-H. Choi, J. Kim, H.-W. Lee, J.-H. Lee, Solid State Ionics 176 (2005) 33–39.
- [9] H. Huang, C.-H. Hsieh, N. Kim, J. Stebbins, F. Prinz, Solid State Ionics 179 (2008) 1442–1445.
- [10] Y. Arachi, T. Asai, O. Yamamoto, Y. Takeda, N. Imanishi, K. Kawate, C. Takakoshi, J. Electrochem. Soc. 148 (2001) A520–A523.
- [11] Z.W. Wang, M.J. Cheng, Y.L. Dong, M. Zhang, J. Power Sources 156 (2006) 306–310.
- [12] D. Meyer, U. Eisele, R. Satet, J. Rödel, Scripta Mater. 58 (2008) 215–218.
- [13] Y.W. Zhang, X. Sun, G. Xu, S.J. Tian, C.S. Liao, C.H. Yan, Phys. Chem. Chem. Phys. 5 (2003) 2129–2134.
- [14] J.T.S. Irvine, J.W.L. Dobson, T. Politova, S.G. Martin, A. Shenouda, Faraday Discuss. 134 (2007) 41–49.
- [15] T.I. Politova, J.T.S. Irvine, Solid State Ionics 168 (2004) 153–165.
- [16] D.P. Fagg, J.C.C. Abrantes, D.P. érez-Coll, P. Núñez, V.V. Kharton, J.R. Frade, Electrochim. Acta 48 (2003) 1023–1029.
- [17] M. Hirano, T. Oka, K. Ukai, Y. Mizutani, Solid State Ionics 158 (2003) 215–223.
- [18] M. Mori, Y. Liu, S.H. Ma, S.I. Hashimoto, K.J. Yasumoto, Electrochemistry 77 (2009) 184–189.